Dynamic and noise properties of multi-electrode tunable semiconductor lasers

Guang-Hua Duan, Philippe Gallion, Jürgen Holtz, Jean-Claude Bouley

J. Phys. III France **2** (1992) 1651-1671 SEPTEMBER **1992,** PAGE 1651

Classification
Physics Abstracts

Dynamic and noise properties of multi-electrode tunable semiconductor lasers

Guang-Hua Duan, Philippe Gallion, Jürgen Holtz and Jean-Claude Bouley (*)

Département Communications, Ecole Nationale Supérieure des Télécommunications, 46 rue Barrault, 75634 Paris Cedex 13, France
(*) Laboratoire de Bagneux, CNET, 196 avenue Henri Ravera, 92220 Bagneux, France

(*Received 18 November 1991, accepted 23 January 1992*)

Abstract. — A general formalism based on the Green's function method is given for multi-electrode semiconductor lasers. The spatial hole burning effect is taken into account in this formalism. The frequency and intensity modulation properties of multi-electrode semiconductor lasers can be predicted using this theory. A general linewidth expression is given which includes contributions from spontaneous emission and carrier shot noise. This method is applied to two-electrode distributed feedback (DFB) and two-electrode distributed Bragg reflector (DBR) lasers. Experimental results for a two-electrode DBR laser are given and show a good agreement with the theoretical model. Moreover, the drive current noise of a tunable multi-electrode laser is shown to have an important influence on the measured lineshape and linewidth.

1. Introduction.

The requirement imposed on sources for coherent optical communication systems has led to the great development of distributed feedback (DFB) and distributed Bragg reflector (DBR) lasers in recent years. The essential feature of these lasers is their ability of dynamic single mode operation. More recently, the requirement of flat FM response and frequency tunability led to the development of multi-electrode lasers [1-7]. The additional electrodes allow for the independent control of, for example, the emission power and the emission frequency [2-6]. The dynamic and noise properties of this type of lasers have also been much affected by the additional electrodes. For example, frequency and amplitude modulation properties can be controlled ; the spontaneous emission rate coupled to the lasing mode is injection current dependent ; carrier shot noise could lead to a non-negligible linewidth, etc.

The main features of multi-electrode lasers are their inherent longitudinal inhomogeneity. Among various classical electromagnetic approaches, the Green's function method initially proposed by Henry [8] is the most efficient in treating spatial inhomogeneities of semiconductor lasers. In this method, the solution of the wave propagation equation corresponding to a point source is called the Green's function. The general solution is a spatial

averaging of the Green's function weighted by the correspondent excitation source. Using this method, the spontaneous emission rate coupled to the lasing mode is related to the laser structure. The phase-amplitude coupling factor is shown to be not only a material parameter, but also affected by the structure and the wavelength detuning from he gain maximum [9]. However these discussions are limited to single electrode lasers.

The dynamic and noise properties of multi-electrode lasers have been analysed first by Lang and Yariv [10]. But in their analysis, the spontaneous emission rate was not related to the laser structure. Moreover, the investigated Cleaved-Coupled-Cavity lasers are of much less interest today. Multi-electrode DFB and DBR lasers have been analysed recently by Tromborg *et al.* using the Green's function method [11, 12]. In their analysis, the Wronskian was considered, for the first time, as a functional of carrier density distribution, rather than as a function of carrier density. This treatment enables the authors to take into account any nonuniform carrier density distribution due to the presence of multi-electrodes and/or due to the spatial hole burning effect. But unfortunately, the Wronskian is considered also as a functional of photon density distribution. This functional dependence is not permitted in the Green's function method, as this method is only valid for a linear dielectric constant. The Wronskian, resulting from solutions of wave equation for a linear dielectric constant, can never be an explicit function of photon density distribution.

The purpose of this paper is to give a comprehensive analysis of multi-electrode lasers. In our approach, the Wronskian is considered as a functional of both frequency and carrier density distribution. The spatial hole burning is included through a power dependent carrier density distribution. The material nonlinear gain can also be taken into account in this method through a perturbation method. That results in an effective nonlinear gain, which is presented in a letter [13]. The full result will be presented in a separate paper [14].

This paper is organized as follows : in section 2, the Green's function method is generalized to multi-electode lasers. In sections 3 and 4 this method is applied to two-electrode DFB and DBR lasers. In section 5, the experimental results for a DBR laser are presented. A conclusion is given at the end of this paper.

2. Theory for multi-electrode semiconductor lasers.

2.1 GENERAL FORMALISM. — The starting point of our analysis is the propagation equation in the frequency domain. It is assumed that the semiconductor medium is linear. This is a good assumption for lasers biased near the threshold. The inclusion of the material nonlinear gain will been presented elsewhere [13, 14]. We shall concentrate our attention to the longitudinal axis, although the same principle of analysis could be used for transverse tuning devices as Tunable-Twin-Guide DFB lasers [15, 16].

In this condition, the electrical field in the laser cavity is thus governed by the inhomogeneous scalar Helmholtz equation [8] :

$$\nabla_z^2 E_\omega(z) + k_0^2\, \varepsilon_\omega(N(z))\, E_\omega(z) = F_\omega(z) \tag{1}$$

where ∇_z^2 is the Laplacian operator for the longitudinal coordinate z, $k_0 = \omega/c$ is the wave number in vacuum, $\varepsilon_\omega(N(z))$ is the dielectrical constant depending on the carrier density distribution $N(z)$ and $F_\omega(z)$ is the Langevin force describing the spontaneous emission. The complex dielectrical constant is written as :

$$\varepsilon_\omega(N(z)) = [n - j(g - \alpha_L)/(2\, k_0)]^2 \tag{2}$$

where n is the refractive index, g is the gain and α_L the internal loss, both in power. n and g are both functions of carrier density distribution $N(z)$.

The general solution of the scalar equation is obtained by using the Green's function formalism and reads [8] :

$$E_\omega(z) = \int_{(L)} G_\omega(z, z')\, F_\omega(z')\, \mathrm{d}z' \tag{3}$$

where the integration is done over the total cavity length. $G_\omega(z, z')$ is the Green's function given by [8] :

$$G_\omega(z, z') = \frac{Z_+(z>)\, Z_-(z<)}{W(\omega, N(z))} \tag{4}$$

where $z> = \max(z, z')$ and $z< = \min(z, z')$, $Z_+(z)$, $Z_-(z)$ are two independent solutions of the homogeneous equation, satisfying the boundary conditions for the left or right facet and $W(\omega, N(z))$ is the Wronskian of these solutions. The Wronskian is a functional of the analysis frequency ω and the carrier density distribution $N(z)$. It is not explicitly dependent on the coordinate z. Our approach is different from that of Tromborg *et al.*, in which the Wronskian is considered also as a functional of photon density distribution [12]. This is not permitted for neither a linear nor a nonlinear-included material dielectric constant. In the linear case, the photon density distribution does not appear explicitly in the dielectric constant, and in turn, in the Wronskian, although it affects the carrier density distribution through the spatial hole burning effect [17]. In the nonlinear case, the Green's function method can not be used directly. A perturbation method, allowing to overcome this difficulty, leads to a different result from that of Tromborg *et al.* [13, 14].

For a laser system, it is important to study the oscillation condition. In the Green's function method, it is expressed by setting the Wronskian of functions $Z_+(z)$ and $Z_-(z)$ to zero. These two functions $Z_+(z)$ and $Z_-(z)$ are then identical to one solution $Z_0(z)$, satisfying the boundary conditions at both facets and representing the longitudinal distribution of the electrical field in the laser cavity.

After finding the longitudinal distribution of the electrical field in the frequency domain $E_\omega(z)$, the next step is to examine the field evolution in the time domain. In order to do that, the frequency and spatial dependences are separated by dividing the electrical field $E_\omega(z)$ by $Z_0(z)$. The first order development of the Wronskian around the operating point gives :

$$W(\omega, N(z)) = \frac{\partial W}{\partial \omega}(\omega - \omega_0) + \int_{(L)} \frac{\partial W}{\partial N} \Delta N(z)\, \mathrm{d}z \tag{5}$$

where ω_0 is the emission frequency and ΔN is the variation of carrier density distribution from the operating point. By using the inverse Fourier-transform, the following rate equation for the complex amplitude $\beta_0(t)$ is obtained [9] :

$$\frac{\mathrm{d}\beta_0}{\mathrm{d}t} = -j \int_{(L)} W_N\, \Delta N(z)\, \mathrm{d}z\, \beta_0(t) + F_{\beta_0}(t) \tag{6}$$

where $W_N = \dfrac{\partial W/\partial N}{\partial W/\partial \omega}$, $\beta_0(t)$ is the slowly varying complex amplitude. F_{β_0} is the Langevin force associated with the complex amplitude in the time domain. The spontaneous emission rate R_{sp} is given by [8] :

$$R_{sp} = \frac{4\,\omega_0^2}{c^3} \frac{\displaystyle\int_{(L)} Z_0^*\, g_0\, n_0\, n_{sp}\, Z_0\, \mathrm{d}z \int_{(L)} Z_0^*\, n_0\, n_{g_0}\, Z_0\, \mathrm{d}z}{|\partial W/\partial \omega|^2}. \tag{7}$$

Passive sections with energy bandgap different from the lasing band don't contribute directly to the spontaneous emission rate.

To know the dynamic and noise properties, one has to use the rate equation for the carrier density in the laser cavity :

$$\frac{dN(z, t)}{dt} = \mathbf{J}(z, t) - R(N(z, t)) - v_g\, g(z, t)\, S(z, t) + F_N(z, t) \tag{8}$$

where $\mathbf{J}(z, t) = J(z, t)/(ed)$, $J(z, t)$ is the current density, e is the electron charge, d is the thickness of the active layer, $S(z, t)$ is the photon density, $R(N(z, t))$ the non-stimulated recombination rate and $F_N(z, t)$ the Langevin force representing the carrier shot noise. The photon density is related to the field intensity distribution by :

$$S(z, t) = C_0 \,|Z_0(z)|^2 P(t), \qquad C_0 = \frac{1}{wd \displaystyle\int_0^L |Z_0(z)|^2 \,dz} \tag{9}$$

where w is the width of the active layer and $P(t)$ is the total photon number in the cavity. It is assumed here that the spatial and temporal dependences of the photon density can be separated. In fact, this is a direct consequence of the linear approximation of the Wronskian made in (5) [14].

The stationary distributions $\bar{N}(z)$, $Z_0(z)$ are self-consistent solutions of the homogenous propagation equation and the stationary carrier rate equation. These distributions are generally power dependent. This is the spatial hole burning effect [17].

The above analysis gives the basis of our formalism. In what follows, it will be used to discuss the dynamic and noise properties of multi-section lasers. It is more practical to convert the field rate equation into the photon number and phase rate equations as follows :

$$\frac{dP}{dt} = 2 \int_{(L)} W_{N_i}\, \Delta N(z)\, dz\, P(t) + F_P(t) \tag{10a}$$

$$\frac{d\phi}{dt} = - \int_{(L)} W_{N_r}\, \Delta N(z)\, dz + F_\phi(t)\,. \tag{10b}$$

The subscripts r, i refer to the real and imaginary parts of the complex parameter respectively. By linearizing the carrier rate equation and using the Fourier transform, the small signal solution is written as :

$$\Delta P(\Omega) = \frac{F_P}{j\Omega - 2\bar{P} \displaystyle\int_{(L)} U_2 A(z)\, |Z_0(z)|^2 \,dz} + \int_{(L)} H_P(z, \Omega)\, (\Delta \mathbf{J} + F_N)\, dz \tag{11a}$$

$$\Delta N(z, \Omega) = \frac{\Delta \mathbf{J}(z, \Omega) + F_N - A(z)\, |Z_0(z)|^2\, \Delta P(\Omega)}{j\Omega + 1/\tau_R} \tag{11b}$$

$$\Delta\omega(\Omega) = \frac{\displaystyle\int_{(L)} U_1 A(z)\, |Z_0(z)|^2 \,dz}{j\Omega - 2\bar{P} \displaystyle\int_{(L)} U_2 A(z)\, |Z_0(z)|^2 \,dz} F_P + F\phi + 2\pi \int_{(L)} H_f(z, \Omega)\, (\Delta \mathbf{J} + F_N)\, dz \tag{11c}$$

where $A(z) = C_0 v_g g_d[\bar{N}(z) - N_0]$, $\bar{P}$ is the average photo number in the laser cavity and τ_R is the local carrier lifetime defined as :

$$\frac{1}{\tau_R} = \frac{\partial R(N(z))}{\partial N(z)}\bigg|_{N(z)=\bar{N}(z)} + C_0 v_g g_d |Z_0(z)|^2 \bar{P} . \tag{12}$$

The functions U_1 and U_2 are defined as :

$$U_1 = \frac{W_{N_r}}{j\Omega + 1/\tau_R} \qquad U_2 = \frac{W_{N_i}}{j\Omega + 1/\tau_R} . \tag{13}$$

The local photon number and frequency modulation transfer functions denoted by $H_P(z, \Omega)$ and $H_f(z, \Omega)$ are given by :

$$H_P(z, \Omega) = \frac{-2\bar{P}U_2}{j\Omega - 2\bar{P}\int_{(L)} U_2 A(z) |Z_0(z)|^2 \, dz} \tag{14a}$$

$$H_f(z, \Omega) = \frac{-j\Omega U_1}{j\Omega - 2\bar{P}\int_{(L)} U_2 A(z) |Z_0(z)|^2 \, dz} U_2 . \tag{14b}$$

In the first part of our formalism (from ω to t), it is assumed that the carrier density distribution $\Delta N(z)$ is a constant in the time domain. This is a reasonable approximation, as the temporal variation of $\Delta N(z)$ is much slower than the optical frequency $\omega_0(2\pi \times 10^{14}$ Hz). On the contrary, the same $\Delta N(z)$ is considered as a varying parameter in the second part (from t to Ω). This is not inconsistent with the first part, as here we are only discussing the slow varying properties ($\Omega/(2\pi) < 100$ GHz).

2 DYNAMIC RESPONSE. — Without loss of generality, the dynamic response for a two section laser will be discussed in this section. The excitation source is the modulation current $\Delta J(z) = \Delta I_1/s_1$, for $z \in$ section I and $\Delta J(z) = \Delta I_2/s_2$, for $z \in$ section II, with s_1 and the section surface. Thus the carrier density variation, the photon number variation and the frequency deviation are given by :

$$\Delta N(z, \Omega) = A_{N_1} \Delta I_1 + A_{N_2} \Delta I_2 \tag{15a}$$

$$\Delta P(\Omega) = A_{P_1} \Delta I_1 + A_{P_2} \Delta I_2 \tag{15b}$$

$$\Delta\omega(\Omega) = A_{\phi_1} \Delta I_1 + A_{\phi_2} \Delta I_2 \tag{15c}$$

where the transfer functions A_{N_1}, A_{N_2}, ... can be obtained directly from equations (11). Using equations (15b) and (15c), the conditions for pure frequency and pure amplitude modulation are given by :

$$\frac{\Delta I_1}{\Delta I_2} = -\frac{\Delta_{P_2}}{\Delta_{P_1}}; \quad \text{for pure FM} \tag{16a}$$

$$\frac{\Delta I_1}{\Delta I_2} = -\frac{\Delta_{\phi_2}}{\Delta_{\phi_1}}; \quad \text{for pure AM} . \tag{16b}$$

The transfer functions A_{P_1}, A_{P_2}, ... are usually modulation frequency-dependent. To get a broadband pure AM or FM, it is necessary to synthesize a network allowing to satisfy the condition (16a) or (16b) [18].

2.3 PHASE NOISE AND SPECTRAL LINEWIDTH. — The Langevin forces representing the spontaneous emission $F_P(\Omega)$, $F_\phi(\Omega)$ are delta-correlated [8] :

$$\langle F_x(\Omega)\, F_x^*(\Omega')\rangle = 2\, D_{xx}\, \delta(\Omega - \Omega')\,, \qquad X = P,\ \phi\,. \tag{17}$$

The non-zero diffusion coefficients are given by [8] :

$$2\, D_{\phi\phi} = R_{sp}/(2\,\bar{P})\,; \qquad 2\, D_{PP} = 2\,\bar{P} R_{sp}\,. \tag{18}$$

The carrier shot noise is assumed to be delta-correlated in time and in space. The correlation relation is found to be [12] :

$$\langle F_N(z,\ \Omega)\, F_N^*(z,\ \Omega')\rangle = 2\, D_{NN}(z,\ \Omega)\, \delta(z - z')\, \delta(\Omega - \Omega') \tag{19a}$$

$$2\, D_{NN}(z,\ \Omega) = 2[v_g\, g n_{sp}\, C_0\, |Z_0(z)|^2\, \bar{P} + R(N(z))] \tag{19b}$$

$$\langle F_P(\Omega)\, F_N(z,\ \Omega')\rangle = 2\, D_{PN}(z,\ \Omega)\, \delta(\Omega - \Omega') \tag{20a}$$

$$2\, D_{PN}(z,\ \Omega) = -\,2\, R_{sp}\, C_0\, |Z_0(z)|^2\, \bar{P}\,. \tag{20b}$$

The frequency variation driven by noise at zero frequency is written as :

$$\Delta\omega = F_\phi + \alpha_{eff}\frac{F_P}{2\,\bar{P}} + 2\,\pi \int_{(L)} H_f(z,\ 0)\, F_N(z,\ 0)\, dz\,. \tag{21}$$

The effective phase-amplitude coupling factor for the linewidth is obtained from (11) and written as :

$$\alpha_{eff} = -\,\frac{\displaystyle\int_{(L)} W_{N_r}\, \tau_R [\bar{N}(z) - N_0]\, |Z_0|^2\, dz}{\displaystyle\int_{(L)} W_{N_i}\, \tau_R [\bar{N}(z) - N_0]\, |Z_0|^2\, dz}\,. \tag{22}$$

The linewidth is given by the value of the power spectrum density of frequency noise at zero frequency divided by $2\,\pi$. The final expression is given by :

$$\Delta\nu = \frac{R_{sp}}{4\,\pi\bar{P}}\,(1 + \alpha_{eff}^2) + 2\,\pi \int_{(L)} |H_f(z,\ 0)|^2\, 2\, D_{NN}(z,\ 0)\, dz$$

$$+ \frac{\alpha_{eff}}{\bar{P}} \int_{(L)} H_f(z,\ 0)\, 2\, D_{PN}(z,\ 0)\, dz\,. \tag{23}$$

The first term is the contribution of phase fluctuations due to spontaneous emission and that of photon number fluctuations *via* the well-known phase-amplitude coupling. The second term is the carrier shot noise contribution. The last term represents the contribution of cross-correlation between the photon number and carrier density. The carrier shot noise induced linewidth has also been pointed out by using other methods [15, 16, 19].

The above discussion completes our formalism on laser dynamics and noise. In the

following two sections, it will be used to study the widely used two-electrode DFB and DBR lasers. To simplify our analysis, it is assumed that the carrier density distribution and the intensity distribution are the same as those at threshold. This assumption is valid for lasers operating not far from threshold.

3. Application to DFB lasers.

A schematic representation of a two-electrode DFB laser is shown in figure 1. The DFB laser consists of a uniform grating and a uniform active layer. The facet reflectivities are assumed to be zero. Using the classical method of solving the coupled wave equation in the laser cavity, the Wronskian of a two-electrode DFB laser is found to be :

$$W(\omega, N_1, N_2) = 8\,\beta_0\,\gamma_1 \frac{\exp(-\gamma_1 L_1)\,\mathrm{sh}\,(\gamma_1 L_1)}{\kappa - j\Gamma_1\, r_{1\,\mathrm{eff}}(\gamma_1)} [r_{1\,\mathrm{eff}}(\gamma_1)\, r_{2\,\mathrm{eff}}(\gamma_2) - 1] \qquad (24)$$

where β_0 is the Bragg wavenumber, κ the coupling coefficient, L_i the length and γ_i the complex wavenumber [9]. The equivalent reflectivity $r_{i\,\mathrm{eff}}(\gamma_i)$ is given by [20] :

$$r_{i\,\mathrm{eff}} = \frac{-j\kappa}{\gamma_i \coth(\gamma_i L_i) - (\alpha_i - j\,\delta_i)} . \qquad (25)$$

The oscillation condition is obtained by setting the Wronskian given in equation (24) to zero. Using the parameters listed in table I, the lasing wavelength is plotted as a function of the injection current I_2 in the second section in figure 2. The parameter is the injection current I_1 in the first section. Two different tuning behaviours are observed. In the current range $I_2 < I_1$, the lasing wavelength increases with increasing injection current. This region is called « red-shifted » region. On the contrary, the lasing wavelength decreases with increasing injection current in the current range $I_2 > I_1$. This region is called « blue-shifted » region. For an uniform injection current ($I_1 = I_2$), the laser behaves as a single section laser possessing no electronic tunability.

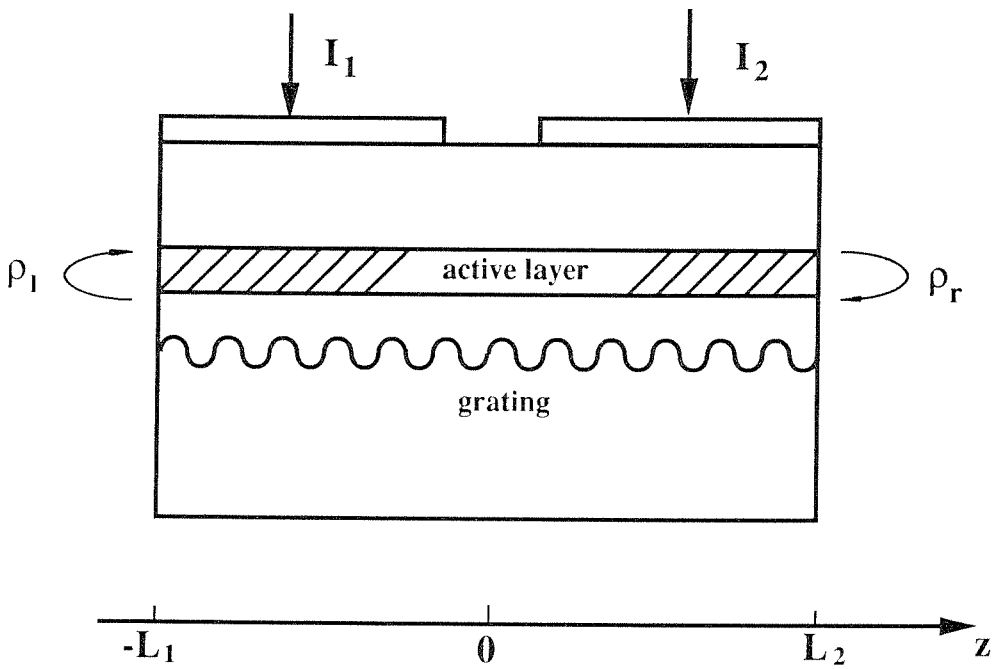

Fig. 1. — Schematic representation of a two-electrode DFB laser.

Table I. — *DFB laser parameters.*

Parameters	Symbols	Values
Length of section 1	L_1	125 μm
Length of section 2	L_2	125 μm
Refractive index in section 1	n_1	3.5
Refractive index in section 2	n_2	3.5
Internal loss (sections 1, 2)	α_{int}	40 cm^{-1}
Factor of Henry (sections 1, 2)	α_H	3.5
Thickness of active layer	—	0.2 μm
Width of active layer	—	1.2 μm
Bragg wavelength	λ_{B0}	1.50 μm
Grating coupling coefficient	κ	50 cm^{-1}
Carrier lifetime in sections 1, 2	τ_{ei}	2 ns
Differential gain (sections 1, 2)	g_{N_i}	1.5×10^{-16} cm^2
Transparent carrier density	N_{0i}	1.0×10^{18} cm^{-3}

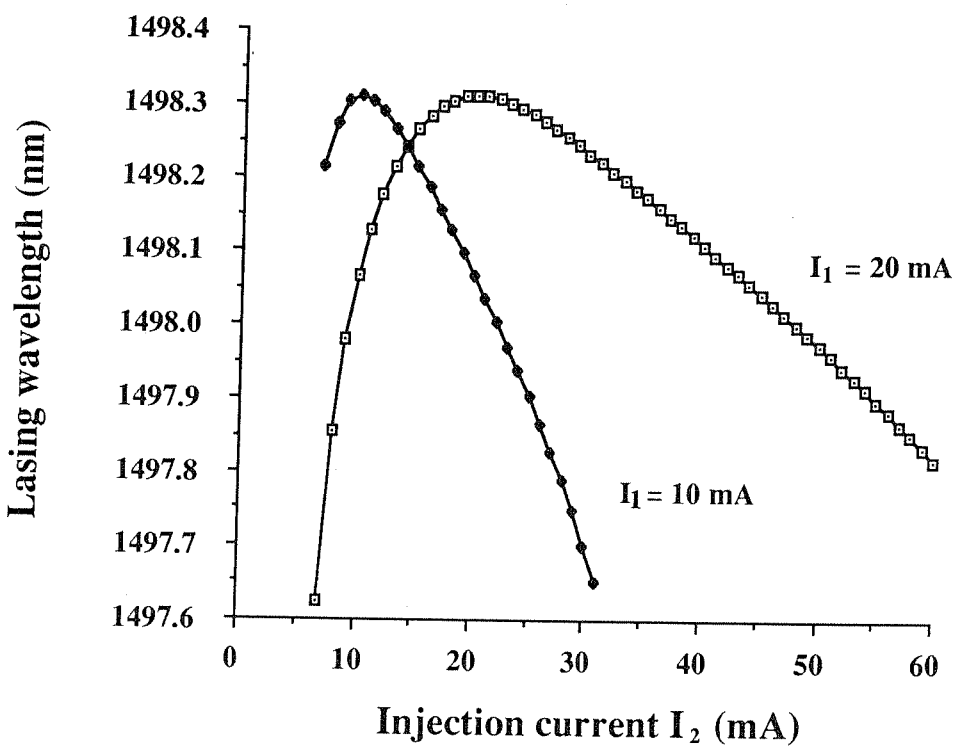

Fig. 2. — Calculated wavelength dependence on the injection current I_2 in the second section of the DFB laser. The parameter is the injection current I_1 in the first section.

By using equation (24), one obtains :

$$\frac{\partial W/\partial N_i}{\partial W/\partial \omega} = \frac{1}{2}\,(-\alpha_{H_i} + j)\, v_{gi}\, g_{di}\, \frac{\tau_{i\,\mathrm{eff}}}{\tau_{\mathrm{eff}}}\, F_i \qquad (26)$$

where α_{H_i} is the material phase-amplitude coupling factor, g_{di} the differential gain, v_{gi} the group velocity and $\tau_{i\,\mathrm{eff}}$ the effective roundtrip time defined by :

$$\tau_{i\,\mathrm{eff}} = \frac{\partial \phi_i}{\partial \omega} \tag{27}$$

and $\tau_{\mathrm{eff}} = \tau_{1\,\mathrm{eff}} + \tau_{2\,\mathrm{eff}}$. Inserting the equation (26) into (10), one can find the dynamic equations for the photon number and the phase of the electrical field. Comparing this formula with that used by Kuznetsov [21], a correction factor F_i appears :

$$F_i = \frac{1 - \dfrac{j}{\tau_{i\,\mathrm{eff}}} \dfrac{\partial \ln |r_{i\,\mathrm{eff}}|}{\partial \omega}}{1 - \dfrac{j}{\tau_{\mathrm{eff}}} \dfrac{\partial \ln |r_{1\,\mathrm{eff}}\, r_{2\,\mathrm{eff}}|}{\partial \omega}}. \tag{28}$$

This correction factor arises from the fact that the dependence of the modulus of the reflectivity on the wavelength affects the frequency modulation properties. However, as the modulus of the effective reflectivity does not change rapidly with the frequency in the positive gain region for an active Bragg section, the resulting correction factor is usually close to unity and can be neglected in many practical cases.

The FM modulation responses in the « blue-shifted » region (I_1 = 20 mA, I_2 = 10 mA) and « red-shifted » region (I_1 = 20 mA, I_2 = 40 mA) are presented in figure 3 showing clearly a difference. In the « red-shifted » region, the FM efficiency is very high but the modulation frequency is limited in the order of 500 MHz. In the « blue-shifted » one, the FM efficiency is low but the cut-off frequency reaches 2 GHz. This results are similar to those of Kuznetsov [21].

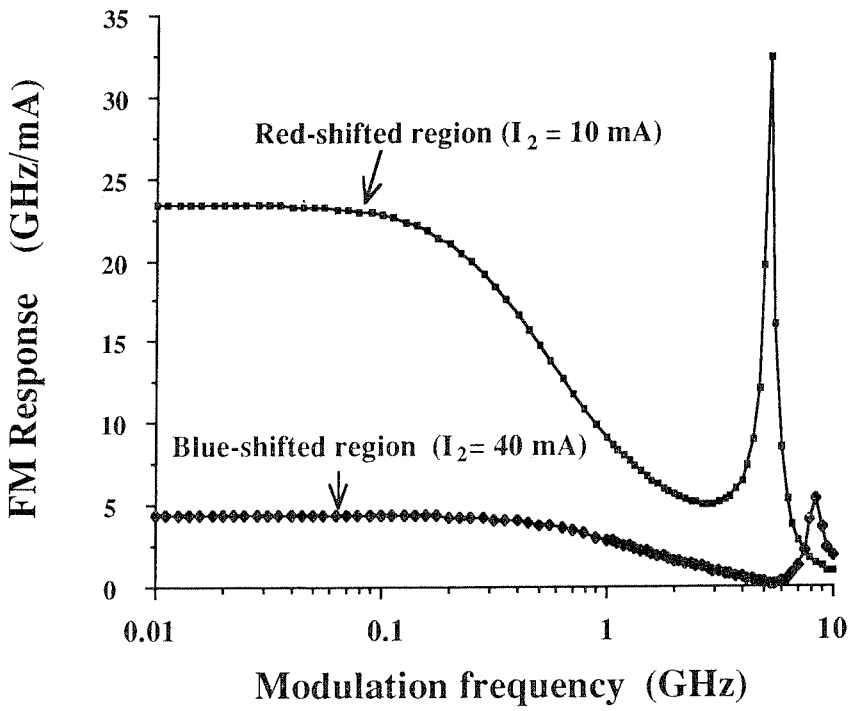

Fig. 3. — FM response in the « red-shifted » region (I_1 = 20 mA, I_2 = 10 mA) and « blue-shifted » region (I_1 = 20 mA, I_2 = 40 mA) of the two-electrode DFB laser. The modulation is only applied to the first section.

It is shown in section (2.2) that pure amplitude modulation and pure frequency modulation can be obtained by an appropriate choice of the current splitting ratio for a given operating point. The optimized FM response and the associated AM response for the operating point, $I_1 = 20$ mA and $I_2 = 40$ mA, is shown in figure 4. The optimized splitting ratio $a = (\Delta I_1/\Delta I_2)$ is found to be -0.396. One can see that the AM response is damped by 50 dB compared to the maximum AM response. Moreover, the optimized AM response and its associated FM response are shown in figure 5 at the same operating point as in figure 4.

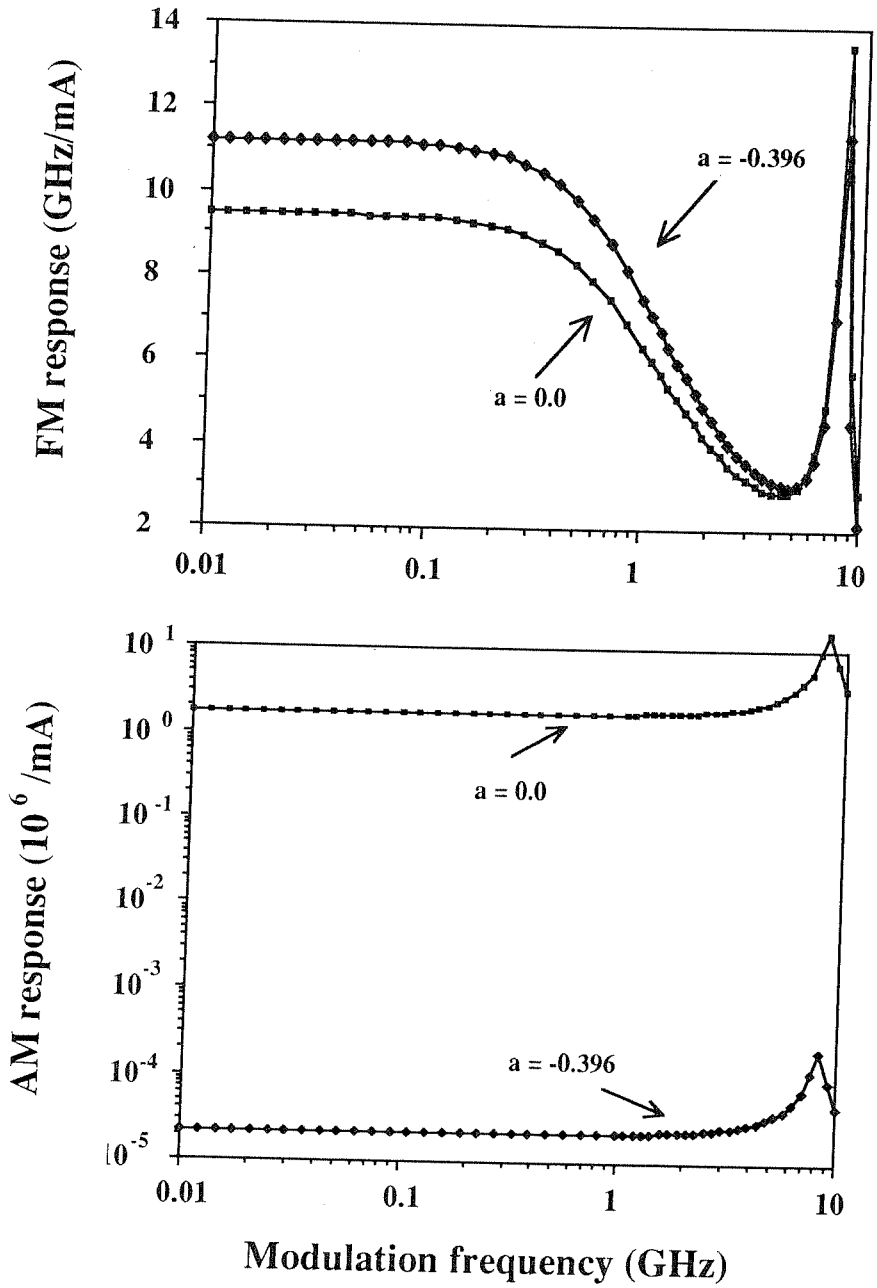

Fig. 4. — Optimized FM response (GHz/mA) and associated AM response (photon number/mA) of the two-electrode DFB laser at the operating point $I_1 = 20$ mA, $I_2 = 40$ mA. The optimized current splitting ratio is found to be $a = -0.396$.

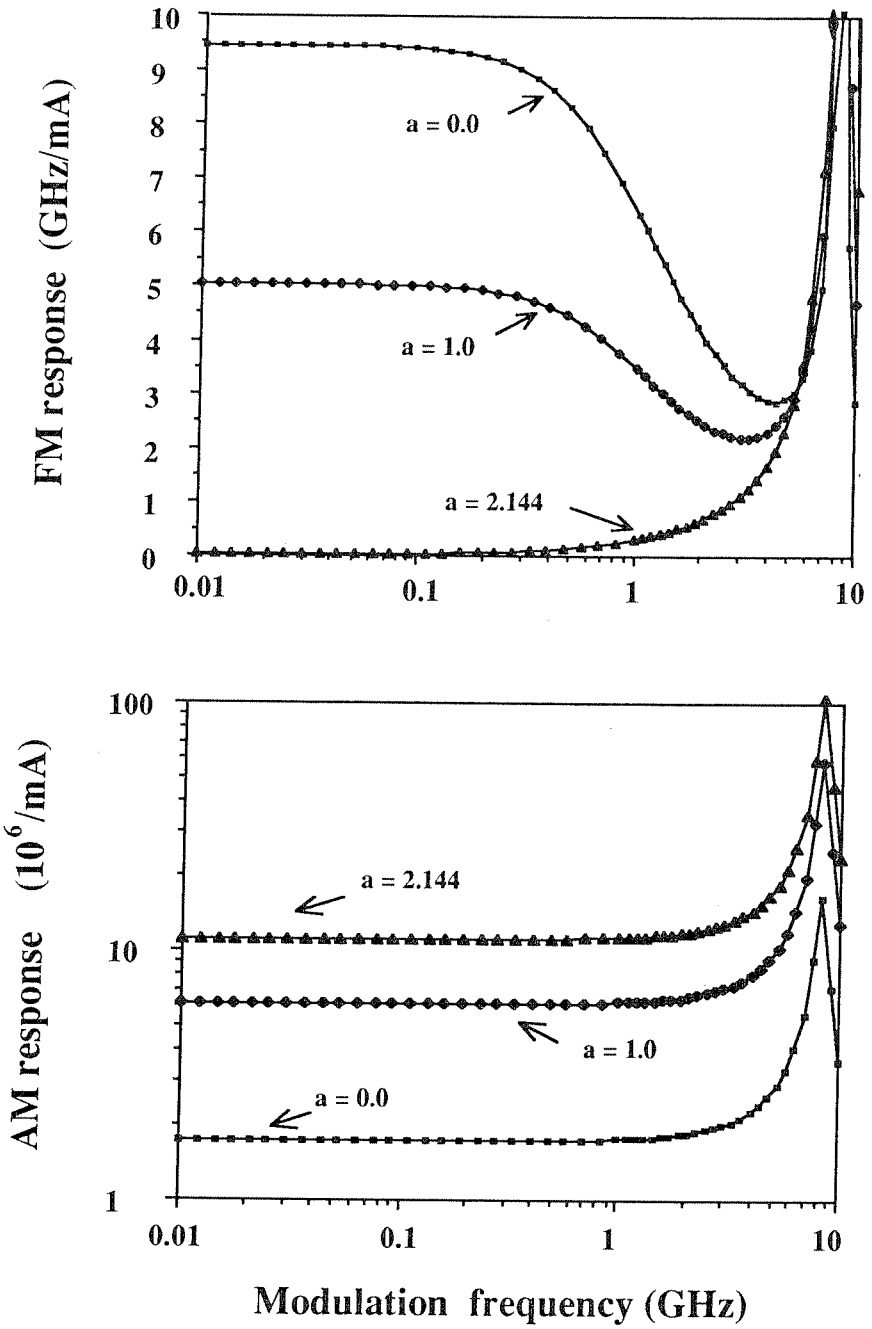

g. 5. — Optimized AM response (photon number/mA) and associated FM response (GHz/mA) of the o-electrode DFB laser at the same operating point as in figure 4. The optimized current splitting ratio found to be $a = 2.144$.

Application to two-electrode DBR lasers.

BR lasers have the advantages of having large tuning range, low linewidth and high FM odulation efficiency. They are suitable for use as local oscillators or transmitters in ultichannel transmission systems.

The DBR laser structure is schematically shown in figure 6. The Wronskian in a DBR laser written as [8, 9] :

$$W(\omega, N_1, N_2) = 2 j\beta_1 r_1 [r_1 r_{\text{eff}} \exp(-2 j\beta_1 L_1) - 1] \tag{29}$$

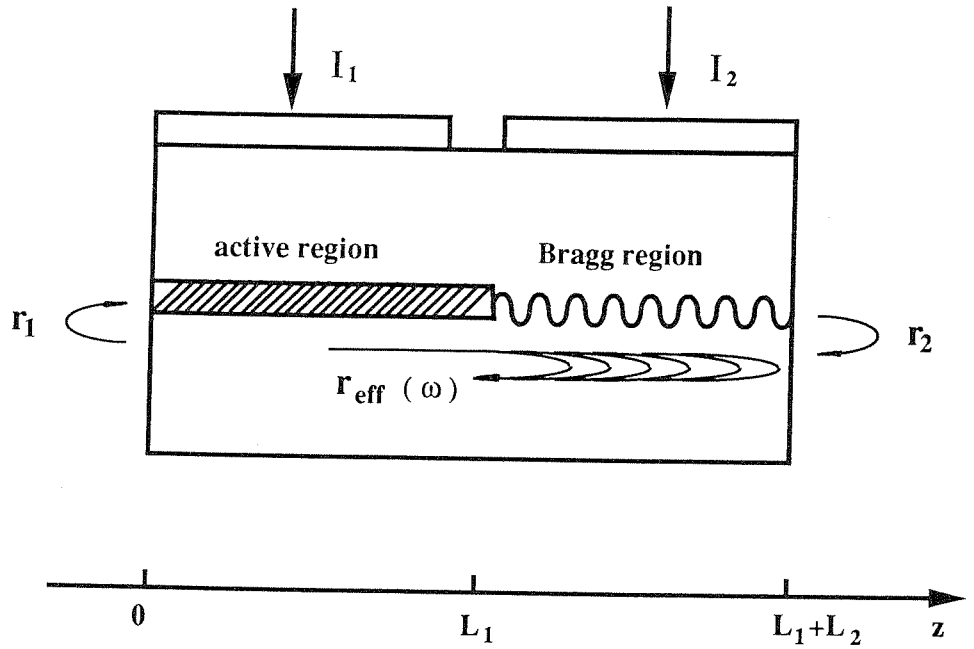

Fig. 6. — Schematic representation of a two-section DBR laser.

where β_1 is the propagation constant, L_1 the length of the active section, and r_1 the reflectivity of the left facet. The effective reflectivity r_{eff} of the Bragg section is given by :

$$r_{\text{eff}} = \frac{-j\kappa C_0}{\gamma_2 \coth(\gamma_2 L_2) - (\alpha_2 - j\delta_2)} \tag{30}$$

where C_0 is the coupling coefficient between the active and the Bragg sections. Other parameters have the same definition as those in the two-electrode DFB laser.

The oscillation condition was discussed previously [9]. The frequency tunability in a DBR laser results from two effects : the variations of the refractive index and of the modulus of the reflectivity in the Bragg section. The latter changes the threshold gain and hence the refractive index in the active section *via* material phase-amplitude coupling. However, as the variation of the Bragg frequency is much faster than that of the mode frequency, DBR lasers without a phase-control region usually have discontinuous tuning characteristics [2].

The dynamic properties in a DBR laser are relatively simple to modelize. Using the results presented in section 2.2 and parameters shown in table II, the FM modulation transfer function is represented in figure 7. For modulation applied to the Bragg section, the FM efficiency is constant at low frequencies up to the cut-off frequency determined by the carrier lifetime in the Bragg section. At frequencies above 1 GHz, FM efficiency of the passive section is enhanced by relaxation oscillation of the carrier density in the active section.

When the modulation is applied to the active section, the FM modulation behaviour is similar to that of single electrode lasers. The FM efficiency due to carrier modulation increases with modulation frequency and reaches its maximum near the relaxation frequency. However, the measured FM response of the active section is quite different from this prediction because of the significant thermal effects at low frequencies.

The contribution of the spontaneous emission to the linewidth has been analysed previously [9]. Adding the carrier shot noise contribution, the linewidth is plotted in figure 8 as a function of tuning current in the Bragg section for an output power of 1 mW. For each mode, the emission frequency changes gradually from positive to negative detuning with respect to

Table II. — *DBR laser parameters.*

Parameters	Symbols	Values
Length of active section	L_1	340 μm
Length of Bragg section	L_2	190 μm
Refractive index in active section	n_1	3.505
Refractive index in Bragg section	n_2	3.2421
Derivative of loss	$d\alpha/dN_2$	$-2{,}5 \times 10^{-17}$ cm^2
Interne loss (active section)	α_{int}	40 cm^{-1}
Reflectivity of left facet	r_1	0.565
Output power	P_1	1 mW
Factor of Henry	α_H	4.0
Derivative of refractive index	dn/dN_2	-6.0×10^{-21} cm^3
Coupling coeff. between two sections	C_0	0.8
Spontaneous emission factor	n_{sp}	2.7
Thickness of active layer	—	0.2 μm
Width of active layer	—	1.2 μm
Recombination coefficient	B	8.0×10^{-11} cm^3/s
Recombination coefficient (Auger)	C	7.5×10^{-29} cm^6/s
Bragg wavelength	λ_B	1.4962 μm
Normalized coupling coefficient	κL_2	5.7 (1,0)
Carrier lifetime in Bragg section	τ_{e2}	2 ns

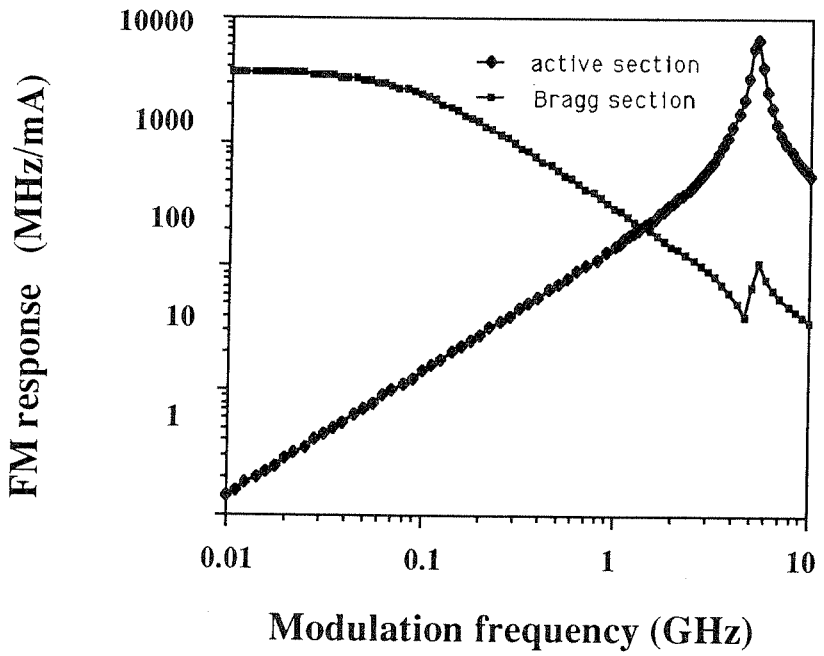

. 7. — FM response of the DBR laser for modulation applied to the active section (a) and to the agg section (b).

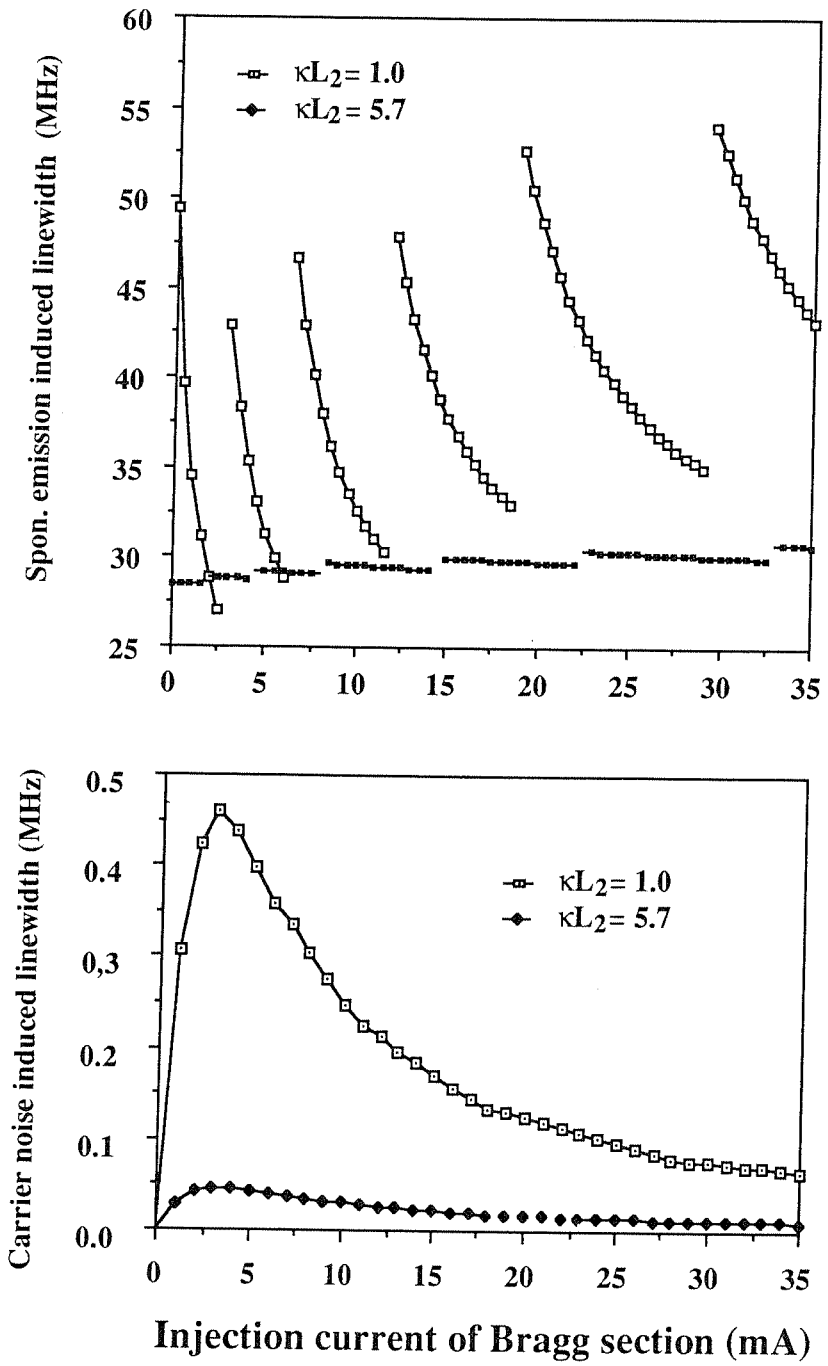

Fig. 8. — (a) Spontaneous emission noise induced linewidth and (b) carrier shot noise induced linewidth as a function of the tuning current. The output power is 1 mW.

the Bragg frequency when the tuning current increases. This leads to a decrease of the effective phase-amplitude coupling factor [9], and in turn, a decrease of the spontaneous emission induced linewidth. In contrast, the carrier shot noise induced linewidth increases for low tuning current and decreases for high tuning current. At an intermediary tuning current, it achieves its maximum [11]. This results from two counteracting variations : the increase of the carrier shot noise and the decrease of frequency tuning efficiency with the tuning current.

Increasing output power reduces the spontaneous emission induced linewidth, but the carrier shot noise induced linewdith is independent of the output power as is shown in

figure 9. The normalized grating coupling coefficient in the Bragg section is assumed to be 1.0. For the laser parameters listed in table II, the carrier noise induced linewidth is smaller than that of the spontaneous emission for normal output power. However, for performant lasers with a sub-megahertz spontaneous emission induced linewidth, the carrier shot noise should be an important limiting factor.

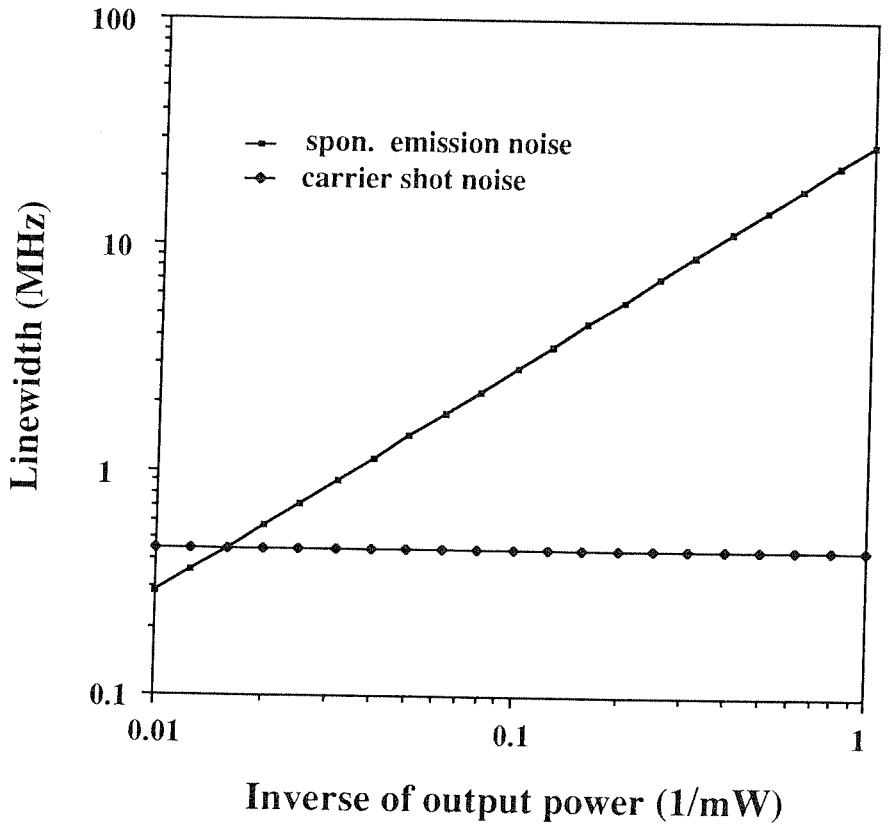

g. 9. — Spontaneous emission noise induced linewidth and carrier shot noise induced linewidth as a nction of inverse of the output power.

Experimental results.

WAVELENGTH TUNING AND FREQUENCY MODULATION CHARACTERISTICS. — The DBR er used in our experiment consists of an active medium InGaAsP with a bandgap at 1.5 μm d a passive waveguide at 1.3 μm. The normalized grating coupling coefficient in the Bragg tion is 5.7. Other parameters are the same as given in table II.

The wavelength variation is plotted in figure 10 as a function of the injection current in the agg section with a constant current $I_1 = 65$ mA for the active section. The wavelength creases with the increasing tuning current I_2. The tuning efficiency varies from 1 to GHz/mA. In the current range 0-70 mA, there are 6 mode jumps. These results are in od agreement with theory [2]. In the mode jump region, the typical hysteresis of velength is measured. For a constant tuning current I_2, the wavelength increases with the ection current in the active section. This tunability results from thermal effects and presents inverse phase with respect to the electronic tunability. The thermal tuning efficiency is ically in the order of 1 GHz/mA.

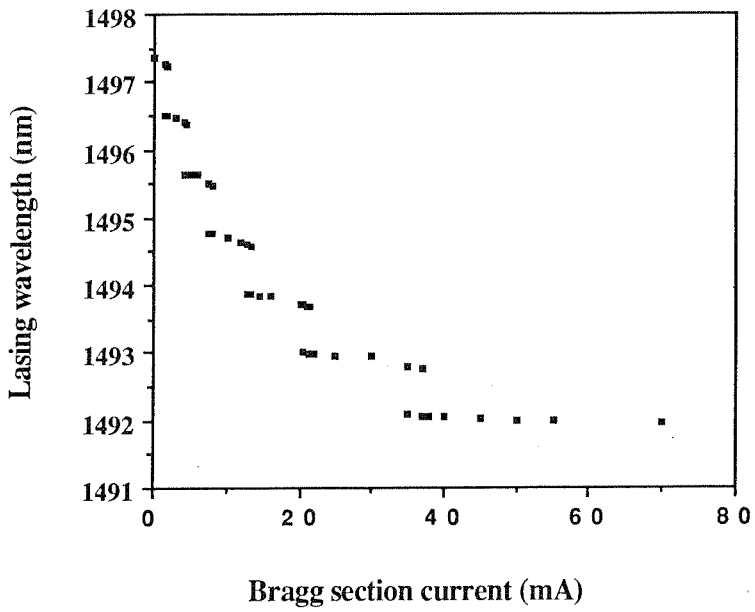

Fig. 10. — Measured tuning characteristics of the DBR laser for a constant current I_1 = 65 mA in the active section.

The FM response is measured by heterodyning two DBR lasers of this type. For modulation applied to the Bragg section the FM sensitivity is shown in figure 11 for two tuning currents. The injection current in the active section is 70 mA. The FM sensitivity remains constant up to the cut-off frequency, which was measured to be 150 MHz. The correspondent carrier lifetime in the Bragg section is about 1.0 ns. The FM sensitivity increases with the tuning current for a given lasing mode.

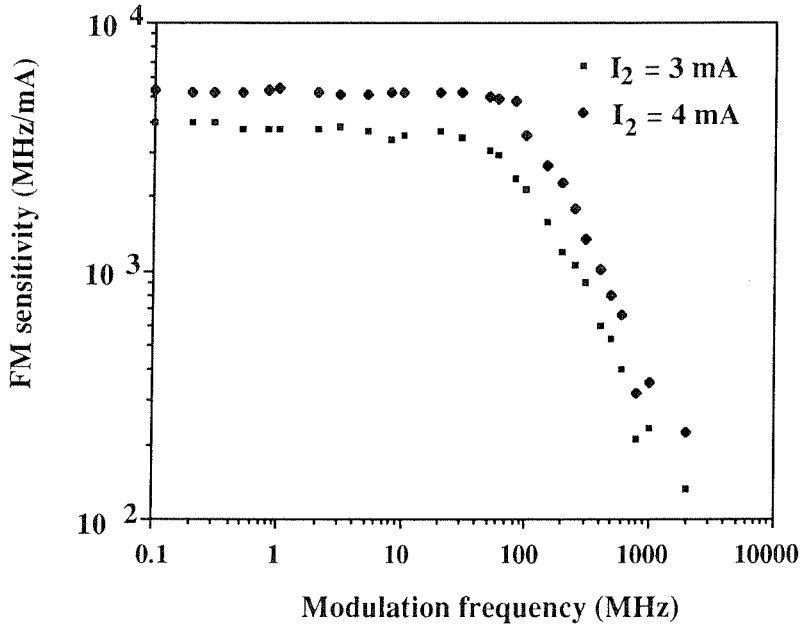

Fig. 11. — Measured FM response of the DBR laser for modulation applied to the Bragg section. The injection current in the active section is 70 mA.

5.2 LINEWIDTH BROADENING DURING WAVELENGTH TUNING. — In previous publications many authors have reported an abnormal increase of the linewidth due to the current injection into the tuning section (see for example Ref. [5]). The increase of the loss due to the current injection in this section tends to broaden the linewidth. However, the magnitude of increase observed is too high to be explained by this cause alone. In the previous sections, it has been shown that the carrier shot noise could contribute to the linewidth, but its magnitude is also much lower than the spontaneous emission noise induced linewidth for the usual DBR laser parameters. On the other hand, it was recently reported by the present authors, that the drive current noise may well be the one of the main sources of the observed linewidth increase [22].

The laser linewidth is measured using a modified delayed self-homodyne technique [23, 24]. The delay line is an 11 km single mode optical fiber. To show the influence of the drive current noise two drive schemes are used for the Bragg section. The first one consists of a standard DC source and a current limiting resistor of 50 Ω. The second one uses an LDX-3620 ultra-low noise current source [22]. The current noise density is about 5.2 nA/ $\sqrt{\text{Hz}}$ at 50 Hz, 815 pA/ $\sqrt{\text{Hz}}$ at 1 kHz and 315 pA/ $\sqrt{\text{Hz}}$ at 25 kHz. The RMS value of the total current fluctuation is about 850 nA. An example of the measured homodyne spectrum is shown in Figure 12. The drive current is 65.0 mA in the active section and 2.2 mA in the Bragg section. The curve (a) represents the measured spectrum using drive scheme 1 and (b) that using drive scheme 2. Curve (a) has a Gaussian shape, whereas (b) is a Lorentzian one, as expected from pure quantum phase noise theory [8]. It has been pointed out that the 3 dB spectral width of a self-homodyne spectrum is twice the spectral linewidth for a Lorentzian shape and $\sqrt{2}$ times the spectral linewidth for a Gaussian shape [23]. Taking this into account, the measured linewidths are 117 MHz with drive scheme 1 and 30 MHz with drive scheme 2.

The Drive Current Noise Induced Linewidth (DCNIL) is obtained by calculating the difference between the measurement results obtained with drives schemes 1 and 2. In Figure 13b, the DCNIL is plotted as a function of the injection current of the Bragg section in

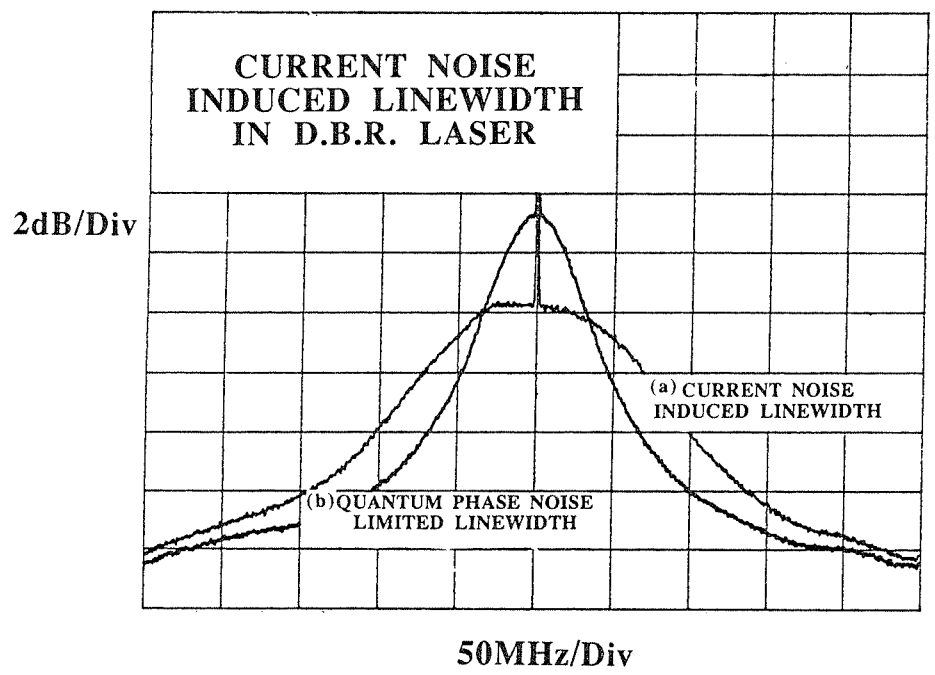

Fig. 12. — Measured homodyne spectrum around the first modulation sideband using two drive schemes. The modulation frequency is 500 MHz. The central peak corresponds to the AM component.

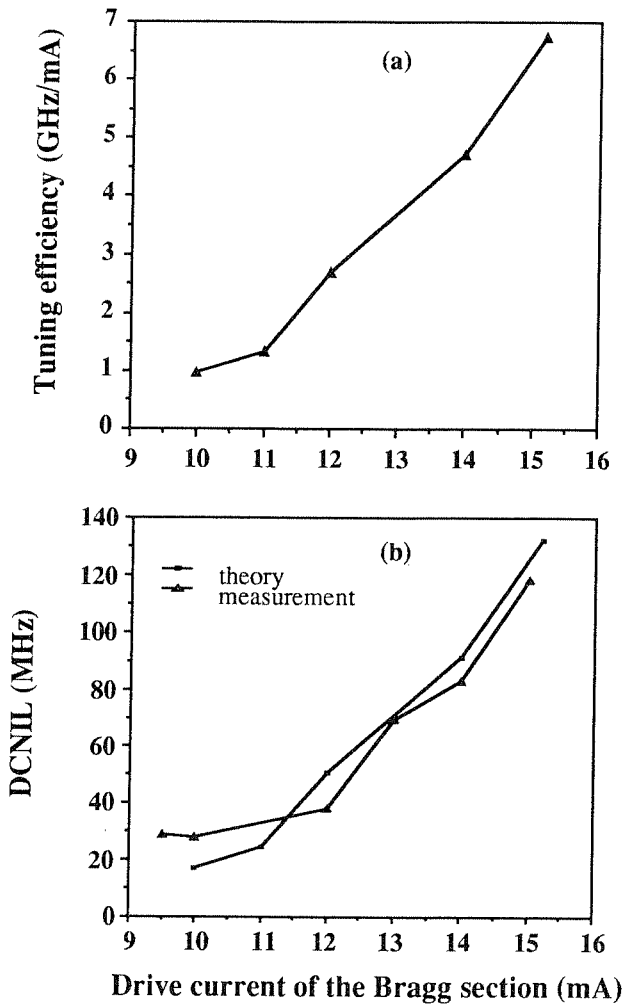

Fig. 13. — (a) Measured tuning efficiency ; (b) measured and calculated linewidth as a function of tuning current. The injection current in the active section is I_1 = 65 mA.

the current range 9.5-15 mA. The tuning efficiency is also shown in figure 13a. The DCNIL and the tuning efficiency increase with tuning current in the Bragg section for a given longitudinal mode of the DBR laser. For other modes the same behaviour is observed.

The DCNIL can be theoretically evaluated. The current noise induced FM noise spectrum $S_f(\Omega)$ is related to the current noise power spectral density $S_I(\Omega)$ by :

$$S_f(\Omega) = |H(\Omega)|^2 S_I(\Omega) \tag{31}$$

where $H(\Omega)$ is the FM transfer function. For a relatively flat current noise spectral density and an FM bandwidth larger than the intrinsic linewidth, the DCNIL is determined by the value of the FM noise spectrum at low frequencies [22]. For most practical cases, the current noise induced FM noise spectrum is of the $1/f$ type. In this case, the resulting power spectrum is approximately a convolution between a Lorentzian intrinsic lineshape and a $1/f$ noise resulted Gaussian lineshape [25-27]. When the $1/f$ noise is the dominant part of the FM noise, the power spectrum is essentially Gaussian. Consider the approximate FM noise spectrum :

$$S_f(\Omega) = H_0^2 K/\Omega \tag{32}$$

where K is a parameter qualifying the current noise level (A^2). The linewidth of the Gaussian

ineshape resulted by this FM noise spectrum is [27] :

$$\Delta\nu_{CN} \approx \frac{H_0}{\pi}\sqrt{\frac{2\,K\ln 2}{\pi}\left(4.3 + \ln\frac{4.3\,H_0^2 K\tau_0^{2.1}}{\pi}\right)} \tag{33}$$

where τ_0 is the delay time of the fiber in the self-homodyne set up. The calculated DCNIL sing the measured tuning efficiency and equation (33) is given in figure 13b. Theory and xperiment are in good agreement using a fitted value K ($= 400\ \mu A^2$). This value is omewhat higher than that estimated by other methods.

After eliminating the influence of DCNIL using a ultra-low noise source LDX-3620, the easured linewidth is plotted as a function of tuning current for $I_1 = 65$ mA in figure 14. The newidth decreases first and becomes constant with the tuning current for a lasing mode, as is xplained in section 4. For other longitudinal modes, the same behaviour is measured.

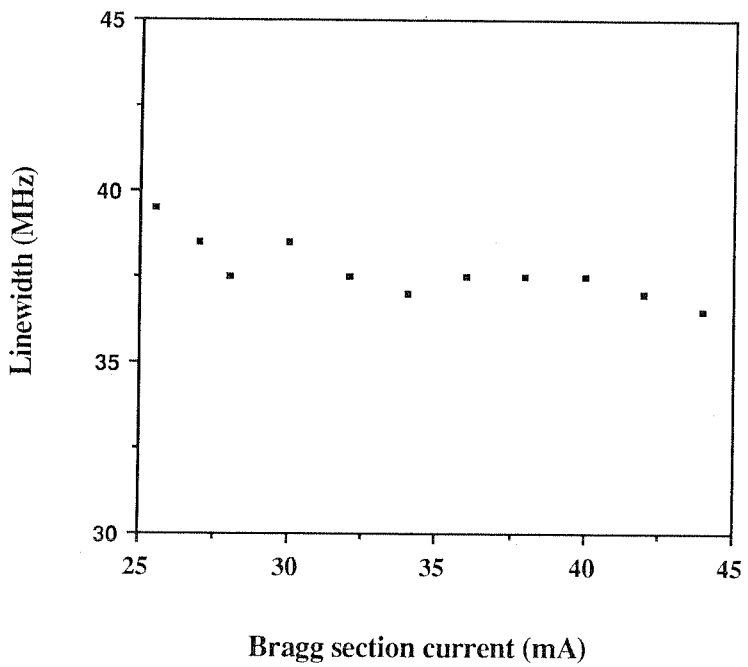

g. 14. — Measured linewidth as a function of tuning current for a constant current $I_1 = 65$ mA in the tive section. An ultra-low noise source is used to bias the tuning section.

Conclusion.

this paper, the Green's function method is extended to multi-electrode tunable niconductor lasers. The evolution of the complex amplitude in the time domain is shown to pend on fluctuations of carrier density distribution. Pure amplitude modulation and pure quency modulation can be obtained by an appropriate choice of modulation current itting ratio. The spontaneous emission coupled to the lasing mode and the effective phase-plitude coupling factor for the linewidth are found to be dependent on stationary carrier nsity distribution. The carrier shot noise leads to a spectral linewidth proportional to the uare of frequency tuning efficiency. The contribution of the correlation between photon

number and carrier density depends on the tuning efficiency and effective phase-amplitude coupling factor.

The Green's function method is applied to a two-electrode DFB laser. The modulation properties in the « red-shifted » and « blue-shifted » regions are discussed. The optimized FM and AM responses are obtained by choosing an appropriate splitting current. The Green's function method is then applied to a two-electrode DBR laser. It is shown that the FM response of the Bragg section is that of a low-pass filter with a cut-off frequency determined by carrier lifetime. The FM response of an active section is typical as for a single electrode laser. The carrier shot noise contribution to the linewidth is of the order of half a megahertz and would be an important limiting factor affecting minimum achievable linewidth.

The drive current noise of the tunable multi-electrode laser is shown to have an important influence on the measured lineshape and linewidth. The current noise usually results in a Gaussian lineshape. The measured DCNIL increases with the increasing frequency tuning efficiency. The previously observed abnormal increase of the linewidth during the wavelength tuning could be explained by this supplementary contribution. The results imply that for tunable multi-electrode lasers ultra-low noise current sources should be used to eliminate the influence of the DCNIL.

Acknowledgment.

The authors wish to thank Professor G. P. Agrawal for useful discussions.

References

[1] KOBAYASHI K. and MITO I., « Single frequency and tunable laser diodes », *IEEE/OSA, J. Lightwave Technol.* **LT-6** (1988) 1623-1633.

[2] KOCH T. L. and KOREN U., « Semiconductor lasers for coherent optical fiber communications », *IEEE/OSA, J. Lightwave Technol.* **LT-8** (1990) 274-293.

[3] BROBERG B. and NILSSON S., « Widely tunable active Bragg reflector integrated lasers in InGaAsP-InP », *Appl. Phys. Lett.* **52** (1988) 1285-1287.

[4] LECLERC D., JACQUET J., SIGOGNE D., LABOURIE C., LOUIS Y., ARTIGUE C. and BENOIT J., « Three-electrode DFB wavelength tunable FSK transmitter at 1.53 μm », *Electron. Lett.* **25** (1989) 45-47.

[5] KOTAKI Y. and ISHIKAWA H., « Spectral characteristics of a three-section wavelength-tunable DBR laser », *IEEE J. Quantum Electron.* **QE-25** (1989) 1340-1345.

[6] MURATA S., MITO I. and KOBAYASHI K., « Spectral characteristics for a 1.5 μm DBR laser with frequency-tuning region », *IEEE J. Quantum Electron.* **QE-23** (1987) 835-838.

[7] ISHIDA O., TOBA H. and TOHMORI Y., « Pure frequency modulation of a multi-electrode distributed-Bragg-reflector (DBR) laser diode », *IEEE Photon. Technol. Lett.* **1** (1989) 156-158.

[8] HENRY C. H., « Theory of spontaneous emission noise in open resonators and its application to lasers and optical amplifiers », *IEEE/OSA J. Lightwave Technol.* **LT-4** (1986) 288-297.

[9] DUAN G. H., GALLION P. and DEBARGE G., « Analysis of the phase-amplitude coupling factor and spectral linewidth of distributed feedback and composite-cavity semiconductor lasers », *IEEE J. Quantum Electron.* **QE-26** (1990) 32-44.

[10] LANG R. J. and YARIV A., « Semiclassical theory of noise in multi-element semiconductor lasers », *IEEE J. Quantum Electron.* **QE-22** (1986) 436-449.

[11] PAN X., OLESEN H. and TROMBORG B., « Spectral linewidth of DFB lasers including the effects of spatial holeburning and nonuniform current injection », *IEEE Photonics Technol. Lett.* **2** (1990) 312-315.

[12] TROMBORG B., OLESEN H. and PAN X., « Theory of linewidth for multi-electrode laser diodes with spatially distributed noise sources », *IEEE J. Quantum Electron.* **QE-27** (1991) 178-192.

[13] DUAN G. H., GALLION P. and AGRAWAL G. P., « Effective nonlinear gain in semiconductor lasers », submitted to *IEEE Photonics Technol. Lett.* **3** (1992) 218-220.

[14] DUAN G. H., GALLION P. and AGRAWAL G. P., « Dynamic and noise properties of semiconductor lasers including nonlinear gain », to appear in *IEEE J. Quantum Electron.*

[15] AMANN M.-C. and SCHIMPE R., « Excess linewidth broadening in wavelength-tunable laser diodes », *Electron. Lett.* **26** (1990) 279-280.

[16] AMANN M.-C. and THULKE W., « Continuously tunable laser diodes : longitudinal *versus* transverse tuning scheme », *IEEE J. Select. Areas Commun.* **SAC-8** (1990) 1169-1177.

[17] WHITEAWAY J. E. A., THOMPSON G. H. B., COLLAR A. J. and ARMISTEAD C. J., « The design and assessment of $\lambda/4$ phase-shifted DFB laser structures », *IEEE J. Quantum Electron.* **QE-25** (1989) 1261-1279.

[18] NILSSON O., GILLNER L. and GOOBAR E., « Formulas for direct frequency modulation response of two-electrode diode lasers : proposals for improvement », *Electron. Lett.* **23** (1987) 1371-1372.

[19] ARNAUD J., « Linewidth of laser diodes with nonuniform phase-amplitude α-factor », *IEEE J. Quantum Electron.* **QE-25** (1989) 668-677.

[20] KUZNETSOV M., « Theory of wavelength tuning in two-segment distributed feedback lasers », *IEEE J. Quantum Electron.* **QE-24** (1988) 1837-1844.

[21] KUZNETSOV M., WILLNER A. E. and KAMINOW I. P., « Frequency modulation response of tunable two-segment distributed feedback lasers », *Appl. Phys. Lett.* **55** (1989) 1826-1828.

[22] DUAN G. H. and GALLION P., « Importance of drive current noise induced linewidth in tunable multi-electrode lasers », *IEEE Photonics Technol. Lett.* **3** (1991) 302-304.

[23] OKOSHI T., KIKUCHI K. and NAKAYAMA A., « Novel method for high resolution measurement of laser output spectrum », *Electron. Lett.* **16** (1980) 630-631.

[24] ESMAN R. D. and GOLDBERG L., « Simple measurement of laser diode spectral linewidth using modulation sidebands », *Electron. Lett.* **24** (1988) 1393-1395.

[25] O'MAHONY M. J. and HENNING I. D., « Semiconductor laser linewidth broadening due to $1/f$ carrier noise », *Electron. Lett.* **19** (1983) 1000-1001.

[26] KIKUCHI K., « Effect of $1/f$-type FM noise on semiconductor-laser linewidth residual in high-power limit », *IEEE J. Quantum Electron.* **25** (1989) 684-688.

[27] MERCER L. B., « $1/f$ frequency noise effects on self-heterodyne linewidth measurements », *IEEE/OSA J. Lightwave Technol.* **LT-9** (1991) 485-493.